MMS Observations of Charge State and Mass Dependent Energization of Heavy Ions During Injections in the Earth's Magnetotail

May 6, 2020

Sam Bingham, I. J. Cohen, B. H. Mauk, D. L. Turner, D. G. Mitchell, S. K. Vines, S. A. Fuselier, R. B. Torbert, and J. L. Burch

JHU Applied Physics Laboratory

sam.bingham@jhuapl.edu

JOHNS HOPKINS
APPLIED PHYSICS LABORATORY

Ion composition and charge state during injections

Understanding charge state and mass composition are important for understanding the energization and source of the plasma sheet

Often, we assume protons are always the dominant species in the plasma sheet, and that "all-ion" type observations (which do not distinguish mass composition) are primarily protons at all energies.

However, observations have shown helium and oxygen are often dominant ion species over H^+ in plasma sheet at highly suprathermal energies (e.g. Mitchell et al., 2018 JGR; Cohen et al., 2017 JGR ; Kronberg et al., 2015 JGR)

Requires an explanation for species dependent energization – is it mass dependent effects (e.g. Speiser trajectories [Nosé 2001 JGR], "pick-up" energization [Delcourt 1994 JGR])? Or simply a higher charge-state [Möbius 1987 magnetotail phys]?

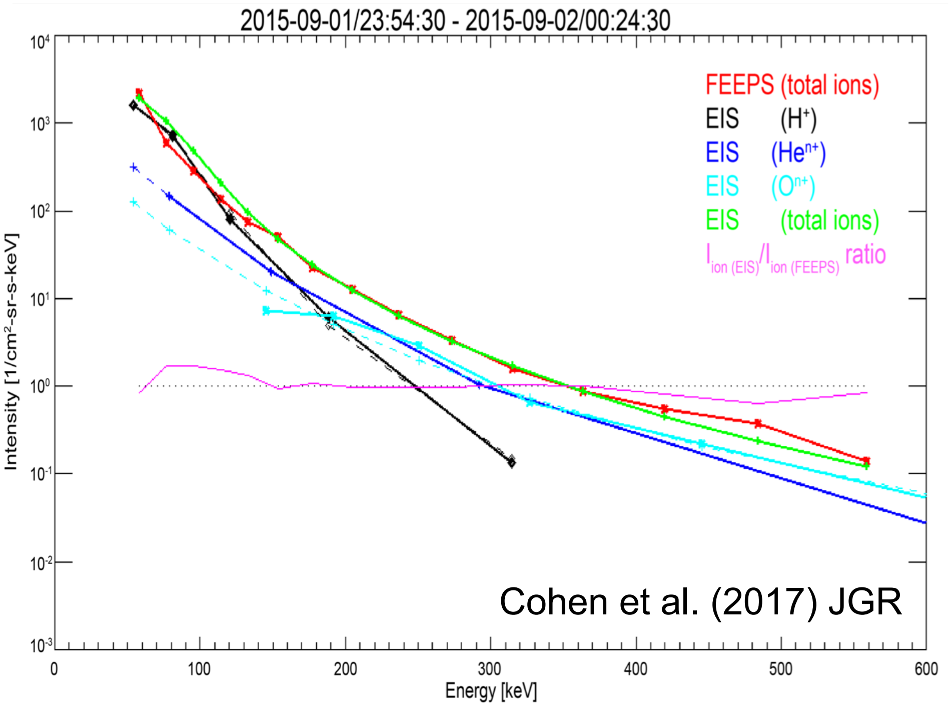

Cohen et al. (2017) JGR

Most recent missions (e.g. Cluster, RBSP, MMS) do not directly measure charge state for ions w/ E > 40 keV/q

i.e. 200 keV O^{6+} and 200 keV O^+ both register as 200 keV oxygen in time-of-flight/solid-state-detector systems

Sam.Bingham@jhuapl.edu

Mitchell et al. (2018) JGR

Ion composition and charge state during injections

Need a way to infer heavy ion charge state!

W/ RBSP-RBSPICE injection observations (inside 6 R_E), Mitchell et al. (2018) used correlation of flux, at different energies to infer the heavy ion charge state

Bounce-averaged guiding center particle motion is dependent on energy/charge

$$\frac{d\boldsymbol{x}}{dt} = \boldsymbol{v}_{E\times B} + \frac{KE_{\perp}}{q}\boldsymbol{v}_{gc},$$

If no mass-dependent effects, ion trajectories and energization is charge-state dependent

By calculating the correlation coefficient between flux of each energy channel for different species, ridges of correlation could reveal the charge state. i.e. strong correlation where E_{heavy} = (heavy charge state)*E_{H+}

How well does this hold up deeper in the tail? Showing 4 examples of observations from MMS, which are representative of 4 types of cases we observe from a larger body injections

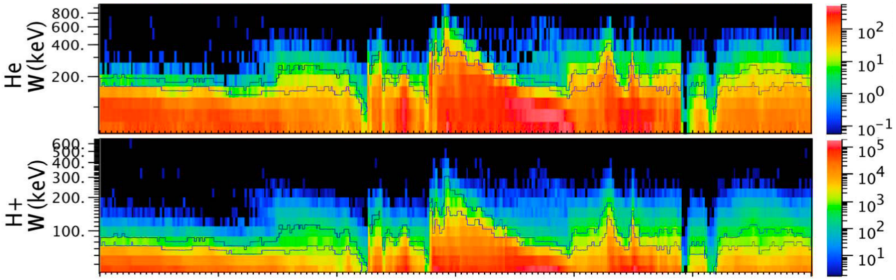

RBSP observations, Helium reaches higher E than H+

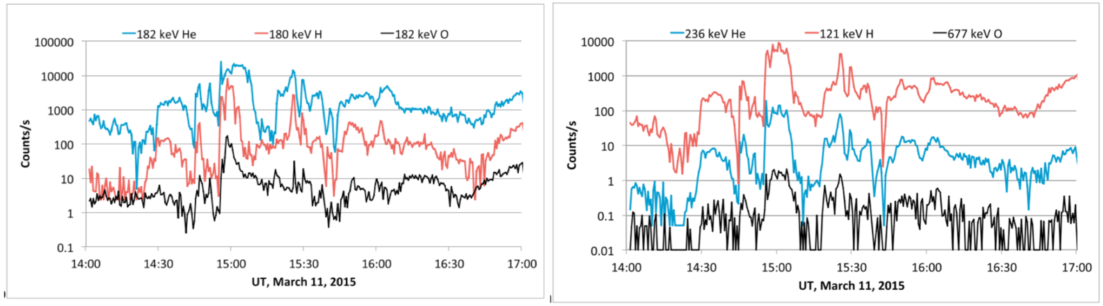

H^+ and He have E dispersions in flux, 236 keV He lines up well with 121 keV H^+, 182 keV He does not line up as well w/ 180 keV H+

H^+ energies

He^{n+} energies

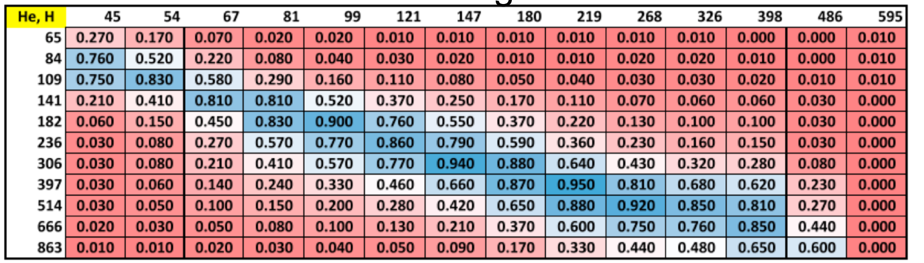

He, H	45	54	67	81	99	121	147	180	219	268	326	398	486	595
65	0.270	0.170	0.070	0.020	0.020	0.010	0.010	0.010	0.010	0.010	0.010	0.000	0.000	0.010
84	0.760	0.520	0.220	0.080	0.040	0.030	0.020	0.010	0.010	0.020	0.020	0.010	0.000	0.010
109	0.750	0.830	0.580	0.290	0.160	0.110	0.080	0.050	0.040	0.030	0.030	0.020	0.010	0.010
141	0.210	0.410	0.810	0.810	0.520	0.370	0.250	0.170	0.110	0.070	0.060	0.060	0.030	0.000
182	0.060	0.150	0.450	0.830	0.900	0.760	0.550	0.370	0.220	0.130	0.100	0.100	0.030	0.000
236	0.030	0.080	0.270	0.570	0.770	0.860	0.790	0.590	0.360	0.230	0.160	0.150	0.030	0.000
306	0.030	0.080	0.210	0.410	0.570	0.770	0.940	0.880	0.640	0.430	0.320	0.280	0.080	0.000
397	0.030	0.060	0.140	0.240	0.330	0.460	0.660	0.870	0.950	0.810	0.680	0.620	0.230	0.000
514	0.030	0.050	0.100	0.150	0.200	0.280	0.420	0.650	0.880	0.920	0.850	0.810	0.270	0.000
666	0.020	0.030	0.050	0.080	0.100	0.130	0.210	0.370	0.600	0.750	0.760	0.850	0.440	0.000
863	0.010	0.010	0.020	0.030	0.040	0.050	0.090	0.170	0.330	0.440	0.480	0.650	0.600	0.000

Corr. Coeffs, Blue cc 1, red cc 0

High correlations where 2*proton energy = helium energy, indicative of He^{2+}

Figures from Mitchell et al. (2018) JGR

Sam.Bingham@jhuapl.edu

To answer, we use MMS EIS Example 1, MMS Observations – 9 R_E

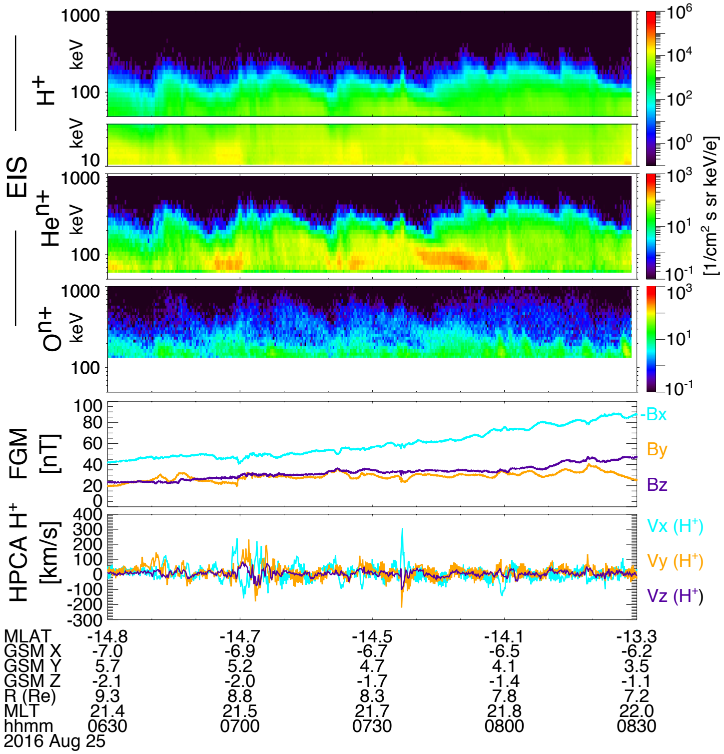

Substorm (*AE*≈500 nT) flows observed by MMS concurrent w/ energetic ion enhancements

He and Oxygen register fluxes at much higher energies than protons

From corr table: Ion fluxes well-correlated indicating He is He^{2+}, and O is O^{6+} for E>~200 keV

He and O reach higher energies than H^+ (>300 keV), due to higher charge state.

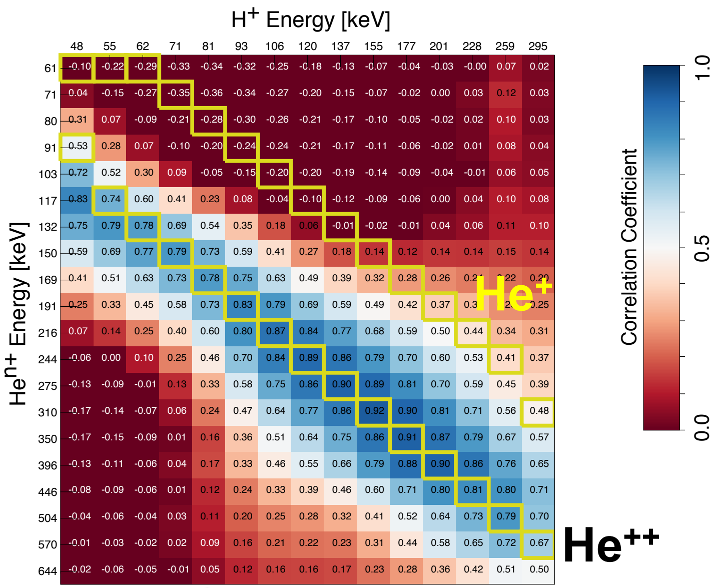

	48	55	62	71	81	93	106	120	137	155	177	201	228	259	295
61	-0.10	-0.22	-0.29	-0.33	-0.34	-0.32	-0.25	-0.18	-0.13	-0.07	-0.04	-0.03	-0.00	0.07	0.02
71	0.04	-0.15	-0.27	-0.35	-0.36	-0.34	-0.27	-0.20	-0.15	-0.07	-0.02	0.00	0.03	0.12	0.03
80	0.31	0.07	-0.09	-0.21	-0.28	-0.30	-0.26	-0.21	-0.17	-0.10	-0.05	-0.02	0.02	0.10	0.03
91	0.53	0.28	0.07	-0.10	-0.20	-0.24	-0.24	-0.21	-0.17	-0.11	-0.06	-0.02	0.01	0.08	0.04
103	0.72	0.52	0.30	0.09	-0.05	-0.15	-0.20	-0.20	-0.19	-0.14	-0.09	-0.04	-0.01	0.06	0.05
117	0.83	0.74	0.60	0.41	0.23	0.08	-0.04	-0.10	-0.12	-0.09	-0.06	0.00	0.04	0.10	0.08
132	0.75	0.79	0.78	0.69	0.54	0.35	0.18	0.06	-0.01	-0.02	-0.01	0.04	0.06	0.11	0.10
150	0.59	0.69	0.77	0.79	0.73	0.59	0.41	0.27	0.18	0.14	0.12	0.14	0.14	0.15	0.14
169	0.41	0.51	0.63	0.73	0.78	0.75	0.63	0.49	0.39	0.32	0.28	0.26	[illegible]	0.22	0.20
191	0.25	0.33	0.45	0.58	0.73	0.83	0.79	0.69	0.59	0.49	0.42	0.37	[illegible]	[illegible]	0.25
216	0.07	0.14	0.25	0.40	0.60	0.80	0.87	0.84	0.77	0.68	0.59	0.50	0.44	0.34	0.31
244	-0.06	0.00	0.10	0.25	0.46	0.70	0.84	0.89	0.86	0.79	0.70	0.60	0.53	0.41	0.37
275	-0.13	-0.09	-0.01	0.13	0.33	0.58	0.75	0.86	0.90	0.89	0.81	0.70	0.59	0.45	0.39
310	-0.17	-0.14	-0.07	0.06	0.24	0.47	0.64	0.77	0.86	0.92	0.90	0.81	0.71	0.56	0.48
350	-0.17	-0.15	-0.09	0.01	0.16	0.36	0.51	0.64	0.75	0.86	0.91	0.87	0.79	0.67	0.57
396	-0.13	-0.11	-0.06	0.04	0.17	0.33	0.46	0.55	0.66	0.79	0.88	0.90	0.86	0.76	0.65
446	-0.08	-0.09	-0.06	0.01	0.12	0.24	0.33	0.39	0.46	0.60	0.71	0.80	0.81	0.80	0.71
504	-0.04	-0.06	-0.04	0.03	0.11	0.20	0.25	0.28	0.32	0.41	0.52	0.64	0.73	0.79	0.70
570	-0.01	-0.03	-0.02	0.02	0.09	0.16	0.21	0.22	0.23	0.31	0.44	0.58	0.65	0.72	0.67
644	-0.02	-0.06	-0.05	-0.01	0.05	0.12	0.16	0.16	0.17	0.23	0.28	0.36	0.42	0.51	0.50

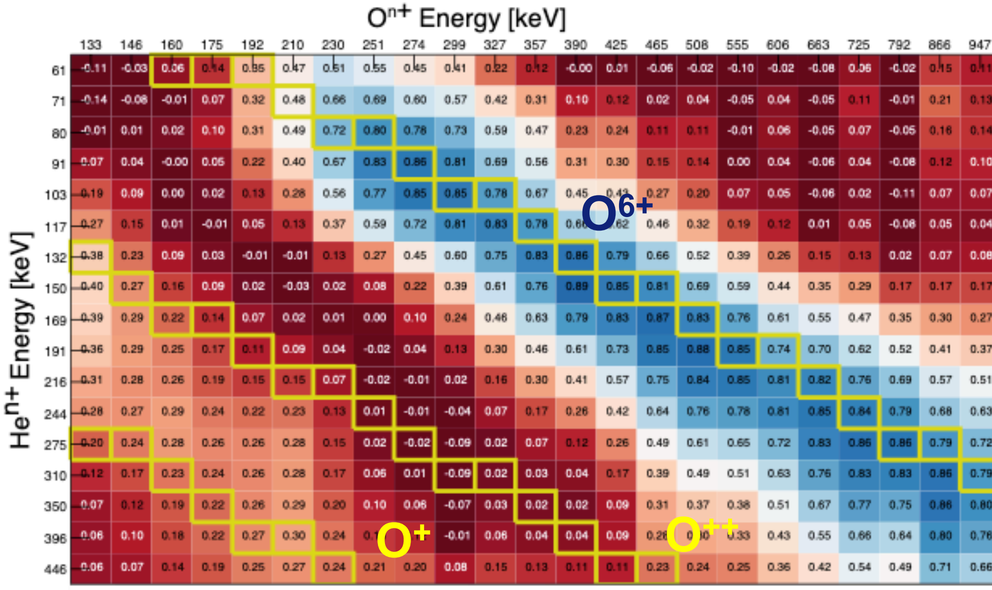

	133	146	160	175	192	210	230	251	274	299	327	357	390	425	465	508	555	606	663	725	792	866	947
61	-0.11	-0.03	0.06	0.14	0.35	0.47	0.51	0.55	0.45	0.41	0.22	0.12	-0.00	0.01	-0.05	-0.02	-0.10	-0.02	-0.08	0.05	-0.02	0.15	0.11
71	-0.14	-0.08	-0.01	0.07	0.32	0.48	0.66	0.69	0.60	0.57	0.42	0.31	0.10	0.12	0.02	0.04	-0.05	0.04	-0.05	0.11	-0.01	0.21	0.13
80	-0.01	0.01	0.02	0.10	0.31	0.49	0.72	0.80	0.78	0.73	0.59	0.47	0.23	0.24	0.11	0.11	-0.01	0.06	-0.05	0.07	-0.05	0.16	0.14
91	0.07	0.04	-0.00	0.05	0.22	0.40	0.67	0.83	0.86	0.81	0.69	0.56	0.31	0.30	0.15	0.14	0.00	0.04	-0.06	0.04	-0.08	0.12	0.10
103	0.19	0.09	0.00	0.02	0.13	0.28	0.56	0.77	0.85	0.85	0.78	0.67	0.45	0.43	0.27	0.20	0.07	0.05	-0.06	0.02	-0.11	0.07	0.07
117	0.27	0.15	0.01	-0.01	0.05	0.13	0.37	0.59	0.72	0.81	0.83	0.78	0.66	0.62	0.46	0.32	0.19	0.12	0.01	0.05	-0.08	0.05	0.04
132	0.38	0.23	0.09	0.03	-0.01	-0.01	0.13	0.27	0.45	0.60	0.75	0.83	0.86	0.79	0.66	0.52	0.39	0.26	0.15	0.13	0.02	0.07	0.08
150	0.40	0.27	0.16	0.09	0.02	-0.03	0.02	0.08	0.22	0.39	0.61	0.76	0.89	0.85	0.81	0.69	0.59	0.44	0.35	0.29	0.17	0.17	0.17
169	0.39	0.29	0.22	0.14	0.07	0.02	0.01	0.00	0.10	0.24	0.46	0.63	0.79	0.83	0.87	0.83	0.76	0.61	0.55	0.47	0.35	0.30	0.27
191	0.36	0.29	0.25	0.17	0.11	0.09	0.04	-0.02	0.04	0.13	0.30	0.46	0.61	0.73	0.85	0.88	0.85	0.74	0.70	0.62	0.52	0.41	0.37
216	0.31	0.28	0.26	0.19	0.15	0.15	0.07	-0.02	-0.01	0.02	0.16	0.30	0.41	0.57	0.75	0.84	0.85	0.81	0.82	0.76	0.69	0.57	0.51
244	0.28	0.27	0.29	0.24	0.22	0.23	0.13	0.01	-0.01	-0.04	0.07	0.17	0.26	0.42	0.64	0.76	0.78	0.81	0.85	0.84	0.79	0.68	0.63
275	0.20	0.24	0.28	0.26	0.26	0.28	0.15	0.02	-0.02	-0.09	0.02	0.07	0.12	0.26	0.49	0.61	0.65	0.72	0.83	0.86	0.86	0.79	0.72
310	0.12	0.17	0.23	0.24	0.26	0.28	0.17	0.06	0.01	-0.09	0.02	0.03	0.04	0.17	0.39	0.49	0.51	0.63	0.76	0.83	0.83	0.86	0.79
350	0.07	0.12	0.19	0.22	0.26	0.29	0.20	0.10	0.06	-0.07	0.03	0.02	0.02	0.09	0.31	0.37	0.38	0.51	0.67	0.77	0.75	0.86	0.80
396	0.06	0.10	0.18	0.22	0.27	0.30	0.24	[illegible]	[illegible]	-0.01	0.06	0.04	0.04	0.09	0.26	[illegible]	0.33	0.43	0.55	0.66	0.64	0.80	0.76
446	0.06	0.07	0.14	0.19	0.25	0.27	0.24	0.21	0.20	0.08	0.15	0.13	0.11	0.11	0.23	0.24	0.25	0.36	0.42	0.54	0.49	0.71	0.66

Sam.Bingham@jhuapl.edu

Example 1, MMS Observations – 9 R_E Comparison of Flux pre/post injection

Pre- and Post-Injection Flux

Pre: 2016-08-25/06:52-06:58
Post: 2016-08-25/07:00-07:10

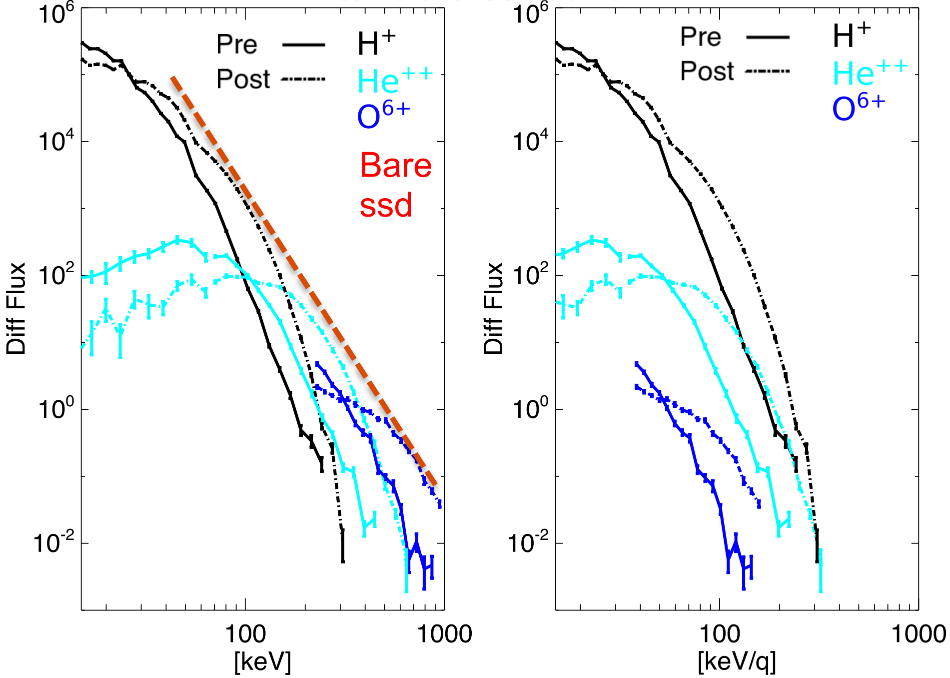

Ratio of Flux Enhancement

Pre: 2016-08-25/06:52-06:58
Post: 2016-08-25/07:00-07:10

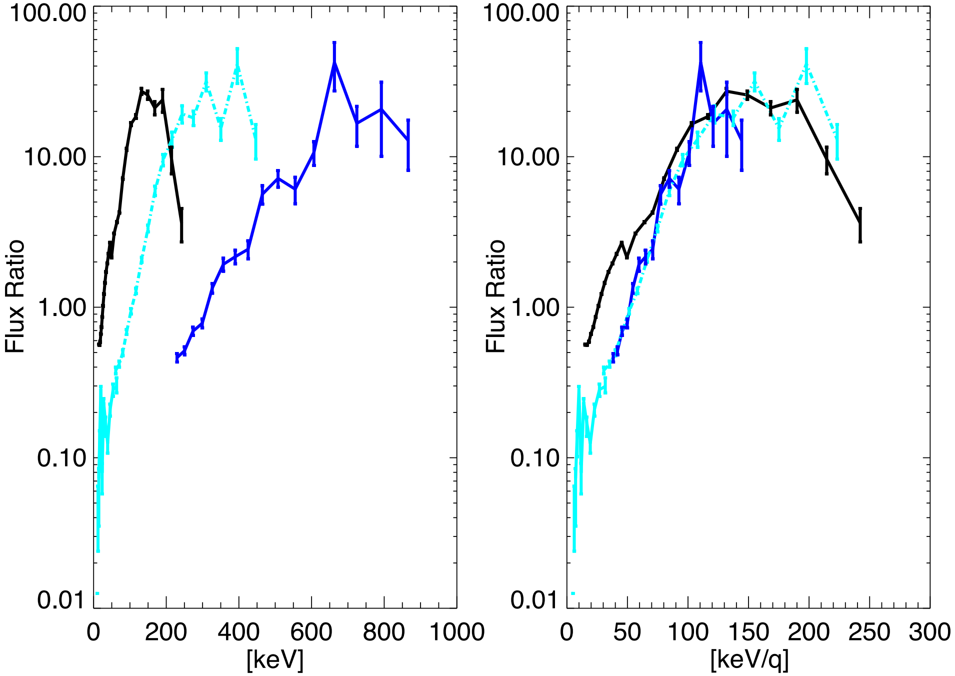

A bare SSD would show ion enhancements to 1 MeV, often would assume all is H^+, actual H+ spectral index is very different!

Composition informs us that high E ions are He and O, if one assumed q=1, would require mass dependent gyromotion to drive greater energization of He and O

Inference of charge-state shows flux and enhancements are best ordered by E/q, matching previous results w/ charge-state [e.g. Möbius 1987] and **indicative E-field driven energization,** which is largely mass independent

Example 2, 9 R_E – separable O^+ and O^{6+}

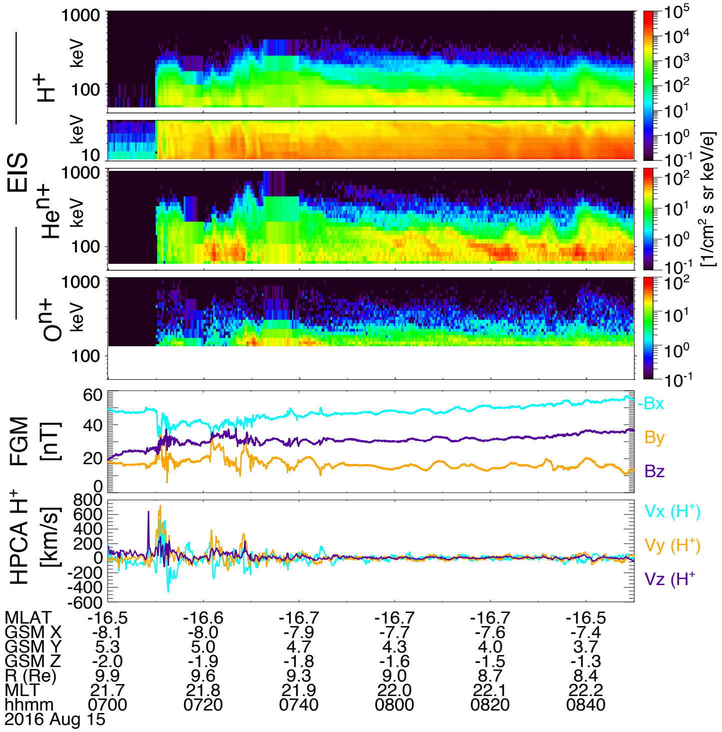

Substorm ($AE \approx 500$ nT) flows observed by MMS during w/ energetic ion enhancements

Ion fluxes well-correlated, corr table indicative of He being He^{2+}, while Oxygen is separable – For E<250 keV O^+, for E>250 keV O^{6+}

Again, He and O that reach higher energies than H^+ (>300 keV), due to higher charge state.

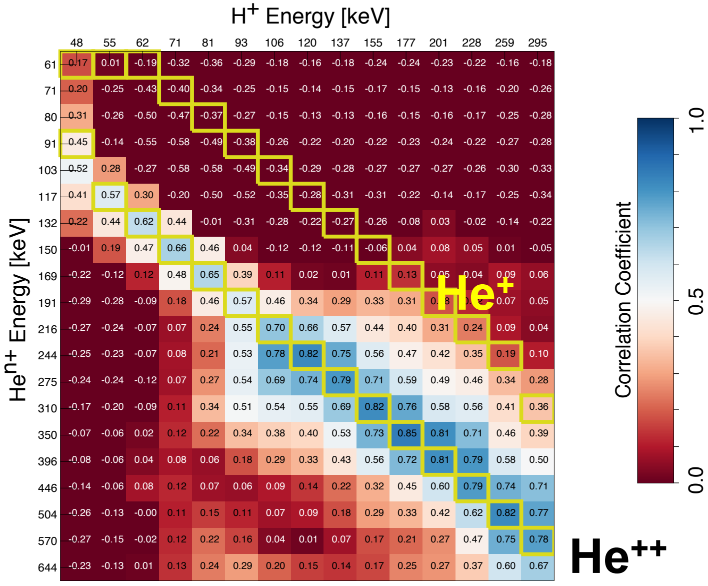

	48	55	62	71	81	93	106	120	137	155	177	201	228	259	295
61	0.17	0.01	-0.19	-0.32	-0.36	-0.29	-0.18	-0.16	-0.18	-0.24	-0.24	-0.23	-0.22	-0.16	-0.18
71	0.20	-0.25	-0.43	-0.40	-0.34	-0.25	-0.15	-0.14	-0.15	-0.17	-0.15	-0.13	-0.16	-0.20	-0.26
80	0.31	-0.26	-0.50	-0.47	-0.37	-0.27	-0.15	-0.13	-0.13	-0.16	-0.15	-0.16	-0.17	-0.25	-0.28
91	0.45	-0.14	-0.55	-0.58	-0.49	-0.38	-0.26	-0.22	-0.20	-0.22	-0.23	-0.24	-0.22	-0.27	-0.28
103	0.52	0.28	-0.27	-0.58	-0.58	-0.49	-0.34	-0.29	-0.28	-0.27	-0.27	-0.27	-0.26	-0.30	-0.33
117	0.41	0.57	0.30	-0.20	-0.50	-0.52	-0.35	-0.28	-0.31	-0.31	-0.22	-0.14	-0.17	-0.25	-0.34
132	0.22	0.44	0.62	0.44	-0.01	-0.31	-0.28	-0.22	-0.27	-0.26	-0.08	0.03	-0.02	-0.14	-0.22
150	-0.01	0.19	0.47	0.66	0.46	0.04	-0.12	-0.12	-0.11	-0.06	0.04	0.08	0.05	0.01	-0.05
169	-0.22	-0.12	0.12	0.48	0.65	0.39	0.11	0.02	0.01	0.11	0.13	0.05	0.04	0.09	0.06
191	-0.29	-0.28	-0.09	0.18	0.46	0.57	0.46	0.34	0.29	0.33	0.31	[illegible]	[illegible]	0.07	0.05
216	-0.27	-0.24	-0.07	0.07	0.24	0.55	0.70	0.66	0.57	0.44	0.40	0.31	0.24	0.09	0.04
244	-0.25	-0.23	-0.07	0.08	0.21	0.53	0.78	0.82	0.75	0.56	0.47	0.42	0.35	0.19	0.10
275	-0.24	-0.24	-0.12	0.07	0.27	0.54	0.69	0.74	0.79	0.71	0.59	0.49	0.46	0.34	0.28
310	-0.17	-0.20	-0.09	0.11	0.34	0.51	0.54	0.55	0.69	0.82	0.76	0.58	0.56	0.41	0.36
350	-0.07	-0.06	0.02	0.12	0.22	0.34	0.38	0.40	0.53	0.73	0.85	0.81	0.71	0.46	0.39
396	-0.08	-0.06	0.04	0.08	0.06	0.18	0.29	0.33	0.43	0.56	0.72	0.81	0.79	0.58	0.50
446	-0.14	-0.06	0.08	0.12	0.07	0.06	0.09	0.14	0.22	0.32	0.45	0.60	0.79	0.74	0.71
504	-0.26	-0.13	-0.00	0.11	0.15	0.11	0.07	0.09	0.18	0.29	0.33	0.42	0.62	0.82	0.77
570	-0.27	-0.15	-0.02	0.12	0.22	0.16	0.04	0.01	0.07	0.17	0.21	0.27	0.47	0.75	0.78
644	-0.23	-0.13	0.01	0.13	0.24	0.29	0.20	0.15	0.14	0.17	0.25	0.27	0.37	0.60	0.67

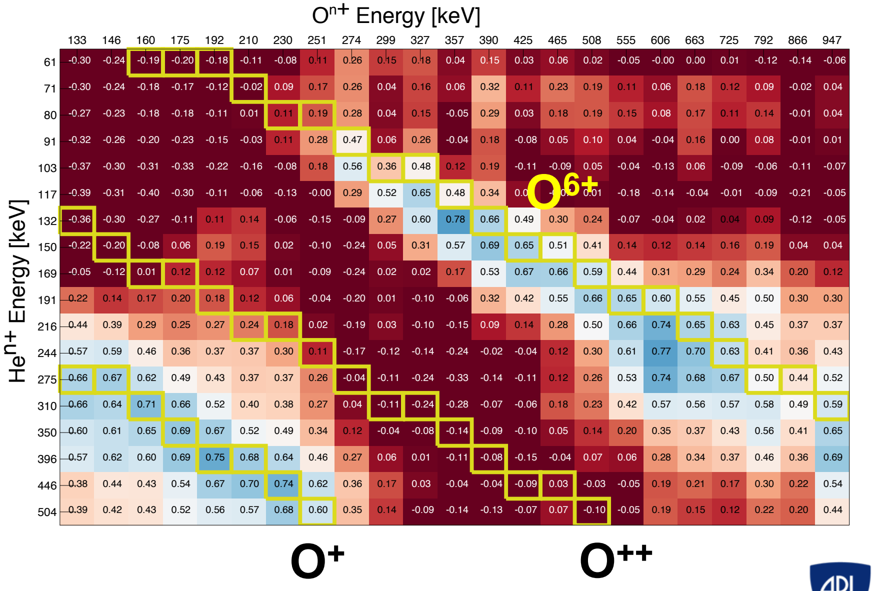

	133	146	160	175	192	210	230	251	274	299	327	357	390	425	465	508	555	606	663	725	792	866	947
61	-0.30	-0.24	-0.19	-0.20	-0.18	-0.11	-0.08	0.11	0.26	0.15	0.18	0.04	0.15	0.03	0.06	0.02	-0.05	-0.00	0.00	0.01	-0.12	-0.14	-0.06
71	-0.30	-0.24	-0.18	-0.17	-0.12	-0.02	0.09	0.17	0.26	0.04	0.16	0.06	0.32	0.11	0.23	0.19	0.11	0.06	0.18	0.12	0.09	-0.02	0.04
80	-0.27	-0.23	-0.18	-0.18	-0.11	0.01	0.11	0.19	0.28	0.04	0.15	-0.05	0.29	0.03	0.18	0.19	0.15	0.08	0.17	0.11	0.14	-0.01	0.04
91	-0.32	-0.26	-0.20	-0.23	-0.15	-0.03	0.11	0.28	0.47	0.06	0.26	-0.04	0.18	-0.08	0.05	0.10	0.04	-0.04	0.16	0.00	0.08	-0.01	0.01
103	-0.37	-0.30	-0.31	-0.33	-0.22	-0.16	-0.08	0.18	0.56	0.36	0.48	0.12	0.19	-0.11	-0.09	0.05	-0.04	-0.13	0.06	-0.09	-0.06	-0.11	-0.07
117	-0.39	-0.31	-0.40	-0.30	-0.11	-0.06	-0.13	-0.00	0.29	0.52	0.65	0.48	0.34	[illegible]	[illegible]	0.01	-0.18	-0.14	-0.04	-0.01	-0.09	-0.21	-0.05
132	-0.36	-0.30	-0.27	-0.11	0.11	0.14	-0.06	-0.15	-0.09	0.27	0.60	0.78	0.66	0.49	0.30	0.24	-0.07	-0.04	0.02	0.04	0.09	-0.12	-0.05
150	-0.22	-0.20	-0.08	0.06	0.19	0.15	0.02	-0.10	-0.24	0.05	0.31	0.57	0.69	0.65	0.51	0.41	0.14	0.12	0.14	0.16	0.19	0.04	0.04
169	-0.05	-0.12	0.01	0.12	0.12	0.07	0.01	-0.09	-0.24	0.02	0.02	0.17	0.53	0.67	0.66	0.59	0.44	0.31	0.29	0.24	0.34	0.20	0.12
191	0.22	0.14	0.17	0.20	0.18	0.12	0.06	-0.04	-0.20	0.01	-0.10	-0.06	0.32	0.42	0.55	0.66	0.65	0.60	0.55	0.45	0.50	0.30	0.30
216	0.44	0.39	0.29	0.25	0.27	0.24	0.18	0.02	-0.19	0.03	-0.10	-0.15	0.09	0.14	0.28	0.50	0.66	0.74	0.65	0.63	0.45	0.37	0.37
244	0.57	0.59	0.46	0.36	0.37	0.37	0.30	0.11	-0.17	-0.12	-0.14	-0.24	-0.02	-0.04	0.12	0.30	0.61	0.77	0.70	0.63	0.41	0.36	0.43
275	0.66	0.67	0.62	0.49	0.43	0.37	0.37	0.26	-0.04	-0.11	-0.24	-0.33	-0.14	-0.11	0.12	0.26	0.53	0.74	0.68	0.67	0.50	0.44	0.52
310	0.66	0.64	0.71	0.66	0.52	0.40	0.38	0.27	0.04	-0.11	-0.24	-0.28	-0.07	-0.06	0.18	0.23	0.42	0.57	0.56	0.57	0.58	0.49	0.59
350	0.60	0.61	0.65	0.69	0.67	0.52	0.49	0.34	0.12	-0.04	-0.08	-0.14	-0.09	-0.10	0.05	0.14	0.20	0.35	0.37	0.43	0.56	0.41	0.65
396	0.57	0.62	0.60	0.69	0.75	0.68	0.64	0.46	0.27	0.06	0.01	-0.11	-0.08	-0.15	-0.04	0.07	0.06	0.28	0.34	0.37	0.46	0.36	0.69
446	0.38	0.44	0.43	0.54	0.67	0.70	0.74	0.62	0.36	0.17	0.03	-0.04	-0.04	-0.09	0.03	-0.03	-0.05	0.19	0.21	0.17	0.30	0.22	0.54
504	0.39	0.42	0.43	0.52	0.56	0.57	0.68	0.60	0.35	0.14	-0.09	-0.14	-0.13	-0.07	0.07	-0.10	-0.05	0.19	0.15	0.12	0.22	0.20	0.44

Example 3, Ex. 25 R_E
Even Deep in the tail PS crossings, fluxes well-correlated by E/q

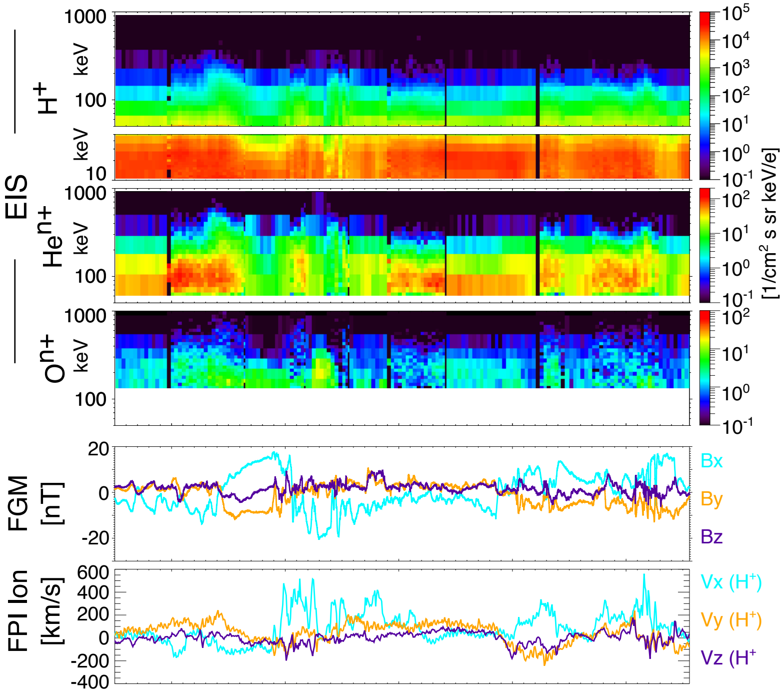

MLAT	-0.9	-1.2	-1.6	-2.0	-2.4
GSM X	-20.9	-20.9	-20.9	-20.9	-20.9
GSM Y	14.1	14.1	14.0	14.0	14.0
GSM Z	1.1	1.1	1.0	1.0	0.9
R (Re)	25.2	25.2	25.2	25.2	25.2
MLT	21.7	21.7	21.7	21.7	21.8
hhmm	0820	0830	0840	0850	0900
2018 Aug 27					

Substorm ($AE \approx 750$ nT) flows observed by MMS during PS crossings w/ energetic ion enhancements

Ion fluxes are still well-correlated between different species for constant E/q. Helium is He^{2+}, ionospheric O^+ up to ~250 keV, solar wind O^{6+} up to an MeV!

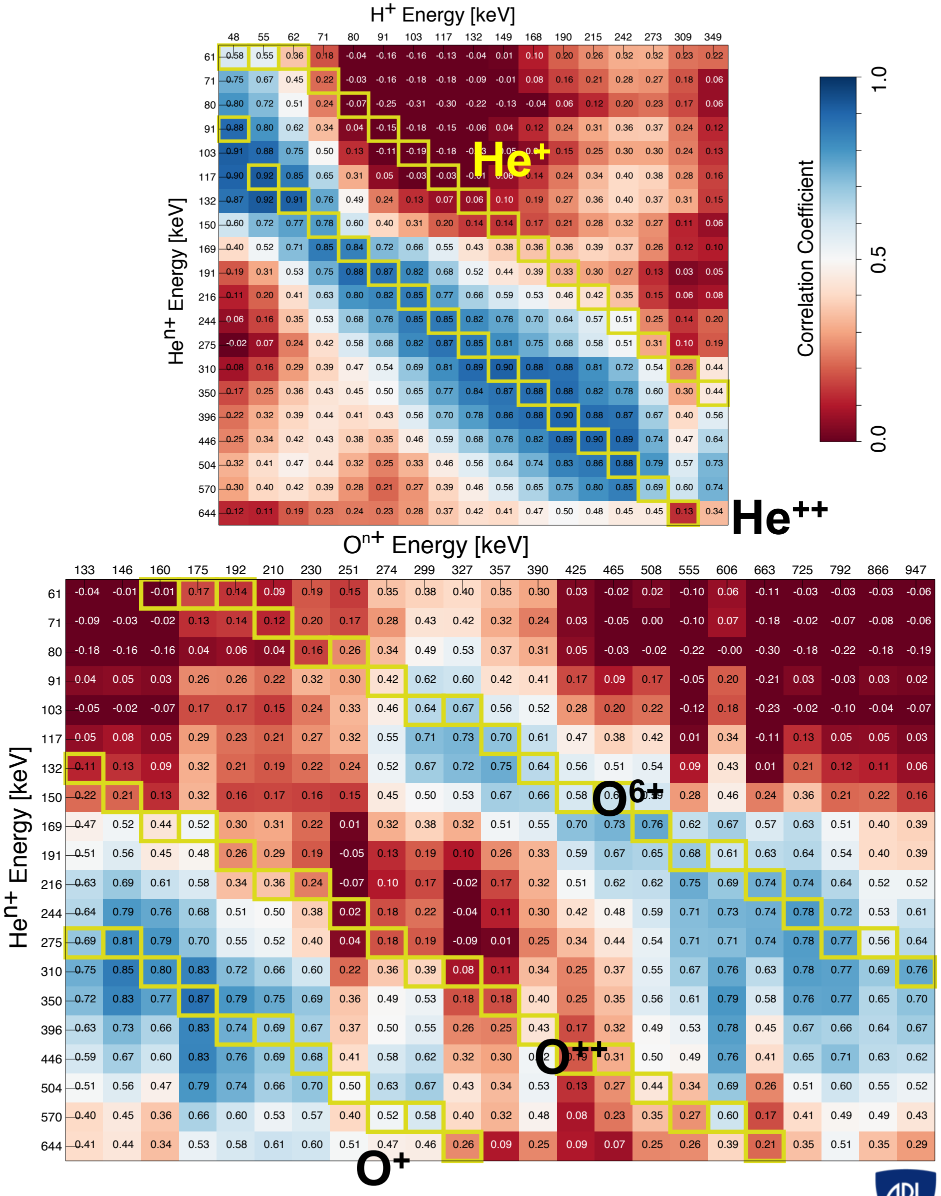

H^+ Energy [keV] (columns) vs. He^{n+} Energy [keV] (rows):

	48	55	62	71	80	91	103	117	132	149	168	190	215	242	273	309	349
61	0.58	0.55	0.36	0.18	-0.04	-0.16	-0.16	-0.13	-0.04	0.01	0.10	0.20	0.26	0.32	0.32	0.23	0.22
71	0.75	0.67	0.45	0.22	-0.03	-0.16	-0.18	-0.18	-0.09	-0.01	0.08	0.16	0.21	0.28	0.27	0.18	0.06
80	0.80	0.72	0.51	0.24	-0.07	-0.25	-0.31	-0.30	-0.22	-0.13	-0.04	0.06	0.12	0.20	0.23	0.17	0.06
91	0.88	0.80	0.62	0.34	0.04	-0.15	-0.18	-0.15	-0.06	0.04	0.12	0.24	0.31	0.36	0.37	0.24	0.12
103	0.91	0.88	0.75	0.50	0.13	-0.11	-0.19	-0.18	[illegible]	0.05	[illegible]	0.15	0.25	0.30	0.30	0.24	0.13
117	0.90	0.92	0.85	0.65	0.31	0.05	-0.03	-0.03	-0.01	0.06	0.14	0.24	0.34	0.40	0.38	0.28	0.16
132	0.87	0.92	0.91	0.76	0.49	0.24	0.13	0.07	0.06	0.10	0.19	0.27	0.36	0.40	0.37	0.31	0.15
150	0.60	0.72	0.77	0.78	0.60	0.40	0.31	0.20	0.14	0.14	0.17	0.21	0.28	0.32	0.27	0.11	0.06
169	0.40	0.52	0.71	0.85	0.84	0.72	0.66	0.55	0.43	0.38	0.36	0.36	0.39	0.37	0.26	0.12	0.10
191	0.19	0.31	0.53	0.75	0.88	0.87	0.82	0.68	0.52	0.44	0.39	0.33	0.30	0.27	0.13	0.03	0.05
216	0.11	0.20	0.41	0.63	0.80	0.82	0.85	0.77	0.66	0.59	0.53	0.46	0.42	0.35	0.15	0.06	0.08
244	0.06	0.16	0.35	0.53	0.68	0.76	0.85	0.85	0.82	0.76	0.70	0.64	0.57	0.51	0.25	0.14	0.20
275	-0.02	0.07	0.24	0.42	0.58	0.68	0.82	0.87	0.85	0.81	0.75	0.68	0.58	0.51	0.31	0.10	0.19
310	0.08	0.16	0.29	0.39	0.47	0.54	0.69	0.81	0.89	0.90	0.88	0.88	0.81	0.72	0.54	0.26	0.44
350	0.17	0.25	0.36	0.43	0.45	0.50	0.65	0.77	0.84	0.87	0.88	0.88	0.82	0.78	0.60	0.30	0.44
396	0.22	0.32	0.39	0.44	0.41	0.43	0.56	0.70	0.78	0.86	0.88	0.90	0.88	0.87	0.67	0.40	0.56
446	0.25	0.34	0.42	0.43	0.38	0.35	0.46	0.59	0.68	0.76	0.82	0.89	0.90	0.89	0.74	0.47	0.64
504	0.32	0.41	0.47	0.44	0.32	0.25	0.33	0.46	0.56	0.64	0.74	0.83	0.86	0.88	0.79	0.57	0.73
570	0.30	0.40	0.42	0.39	0.28	0.21	0.27	0.39	0.46	0.56	0.65	0.75	0.80	0.85	0.69	0.60	0.74
644	0.12	0.11	0.19	0.23	0.24	0.23	0.28	0.37	0.42	0.41	0.47	0.50	0.48	0.45	0.45	0.13	0.34

O^{n+} Energy [keV] (columns) vs. He^{n+} Energy [keV] (rows):

	133	146	160	175	192	210	230	251	274	299	327	357	390	425	465	508	555	606	663	725	792	866	947
61	-0.04	-0.01	-0.01	0.17	0.14	0.09	0.19	0.15	0.35	0.38	0.40	0.35	0.30	0.03	-0.02	0.02	-0.10	0.06	-0.11	-0.03	-0.03	-0.03	-0.06
71	-0.09	-0.03	-0.02	0.13	0.14	0.12	0.20	0.17	0.28	0.43	0.42	0.32	0.24	0.03	-0.05	0.00	-0.10	0.07	-0.18	-0.02	-0.07	-0.08	-0.06
80	-0.18	-0.16	-0.16	0.04	0.06	0.04	0.16	0.26	0.34	0.49	0.53	0.37	0.31	0.05	-0.03	-0.02	-0.22	-0.00	-0.30	-0.18	-0.22	-0.18	-0.19
91	0.04	0.05	0.03	0.26	0.26	0.22	0.32	0.30	0.42	0.62	0.60	0.42	0.41	0.17	0.09	0.17	-0.05	0.20	-0.21	0.03	-0.03	0.03	0.02
103	-0.05	-0.02	-0.07	0.17	0.17	0.15	0.24	0.33	0.46	0.64	0.67	0.56	0.52	0.28	0.20	0.22	-0.12	0.18	-0.23	-0.02	-0.10	-0.04	-0.07
117	0.05	0.08	0.05	0.29	0.23	0.21	0.27	0.32	0.55	0.71	0.73	0.70	0.61	0.47	0.38	0.42	0.01	0.34	-0.11	0.13	0.05	0.05	0.03
132	0.11	0.13	0.09	0.32	0.21	0.19	0.22	0.24	0.52	0.67	0.72	0.75	0.64	0.56	0.51	0.54	0.09	0.43	0.01	0.21	0.12	0.11	0.06
150	0.22	0.21	0.13	0.32	0.16	0.17	0.16	0.15	0.45	0.50	0.53	0.67	0.66	0.58	[illegible]	0.59	0.28	0.46	0.24	0.36	0.21	0.22	0.16
169	0.47	0.52	0.44	0.52	0.30	0.31	0.22	0.01	0.32	0.38	0.32	0.51	0.55	0.70	0.73	0.76	0.62	0.67	0.57	0.63	0.51	0.40	0.39
191	0.51	0.56	0.45	0.48	0.26	0.29	0.19	-0.05	0.13	0.19	0.10	0.26	0.33	0.59	0.67	0.65	0.68	0.61	0.63	0.64	0.54	0.40	0.39
216	0.63	0.69	0.61	0.58	0.34	0.36	0.24	-0.07	0.10	0.17	-0.02	0.17	0.32	0.51	0.62	0.62	0.75	0.69	0.74	0.74	0.64	0.52	0.52
244	0.64	0.79	0.76	0.68	0.51	0.50	0.38	0.02	0.18	0.22	-0.04	0.11	0.30	0.42	0.48	0.59	0.71	0.73	0.74	0.78	0.72	0.53	0.61
275	0.69	0.81	0.79	0.70	0.55	0.52	0.40	0.04	0.18	0.19	-0.09	0.01	0.25	0.34	0.44	0.54	0.71	0.71	0.74	0.78	0.77	0.56	0.64
310	0.75	0.85	0.80	0.83	0.72	0.66	0.60	0.22	0.36	0.39	0.08	0.11	0.34	0.25	0.37	0.55	0.67	0.76	0.63	0.78	0.77	0.69	0.76
350	0.72	0.83	0.77	0.87	0.79	0.75	0.69	0.36	0.49	0.53	0.18	0.18	0.40	0.25	0.35	0.56	0.61	0.79	0.58	0.76	0.77	0.65	0.70
396	0.63	0.73	0.66	0.83	0.74	0.69	0.67	0.37	0.50	0.55	0.26	0.25	0.43	0.17	0.32	0.49	0.53	0.78	0.45	0.67	0.66	0.64	0.67
446	0.59	0.67	0.60	0.83	0.76	0.69	0.68	0.41	0.58	0.62	0.32	0.30	[illegible]	0.19	0.31	0.50	0.49	0.76	0.41	0.65	0.71	0.63	0.62
504	0.51	0.56	0.47	0.79	0.74	0.66	0.70	0.50	0.63	0.67	0.43	0.34	0.53	0.13	0.27	0.44	0.34	0.69	0.26	0.51	0.60	0.55	0.52
570	0.40	0.45	0.36	0.66	0.60	0.53	0.57	0.40	0.52	0.58	0.40	0.32	0.48	0.08	0.23	0.35	0.27	0.60	0.17	0.41	0.49	0.49	0.43
644	0.41	0.44	0.34	0.53	0.58	0.61	0.60	0.51	0.47	0.46	0.26	0.09	0.25	0.09	0.07	0.25	0.26	0.39	0.21	0.35	0.51	0.35	0.29

Example 4, ~8 R_E
Non-adiabatic Oxygen Energization

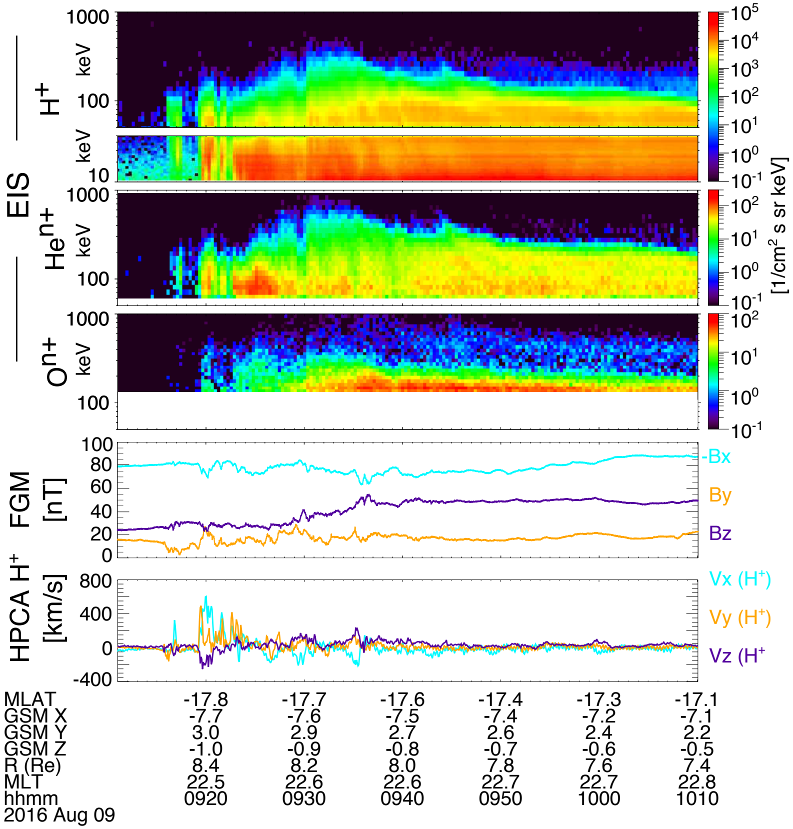

HPCA observes no O^{2+} < 80 keV (40 keV/q)
Most likely, just O^+

Possible source of this extra O^+ energization is "pick-up" energization from induced E-field, e.g. Delcourt et al. (2002) JASTP.

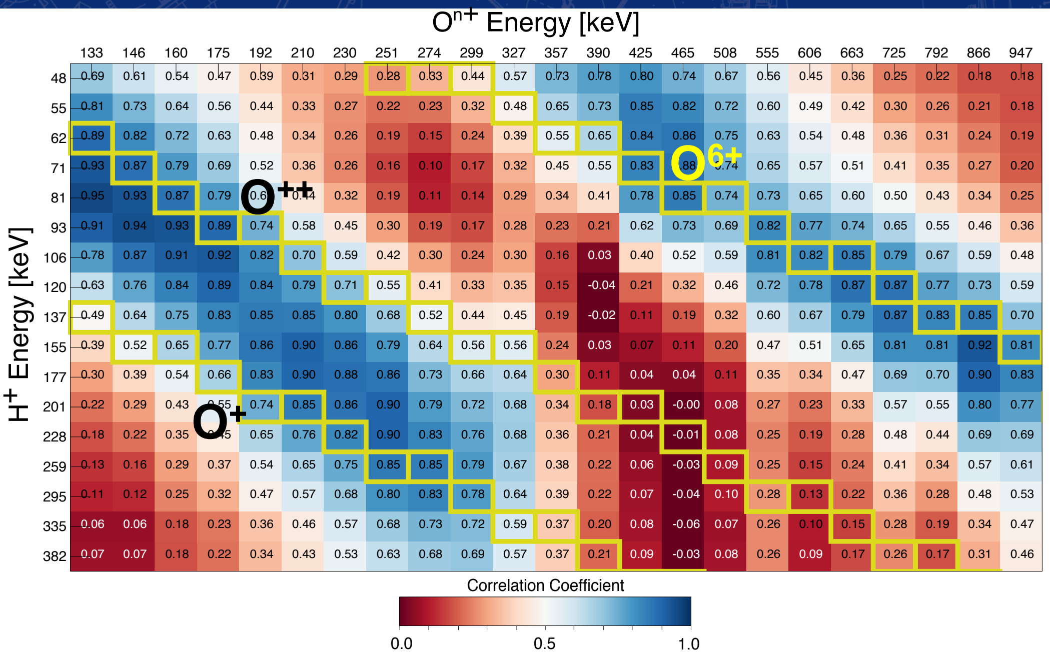

O^{n+} Energy [keV]

H^+ Energy [keV]

	133	146	160	175	192	210	230	251	274	299	327	357	390	425	465	508	555	606	663	725	792	866	947
48	0.69	0.61	0.54	0.47	0.39	0.31	0.29	0.28	0.33	0.44	0.57	0.73	0.78	0.80	0.74	0.67	0.56	0.45	0.36	0.25	0.22	0.18	0.18
55	0.81	0.73	0.64	0.56	0.44	0.33	0.27	0.22	0.23	0.32	0.48	0.65	0.73	0.85	0.82	0.72	0.60	0.49	0.42	0.30	0.26	0.21	0.18
62	0.89	0.82	0.72	0.63	0.48	0.34	0.26	0.19	0.15	0.24	0.39	0.55	0.65	0.84	0.86	0.75	0.63	0.54	0.48	0.36	0.31	0.24	0.19
71	0.93	0.87	0.79	0.69	0.52	0.36	0.26	0.16	0.10	0.17	0.32	0.45	0.55	0.83	.88	0.74	0.65	0.57	0.51	0.41	0.35	0.27	0.20
81	0.95	0.93	0.87	0.79	0.6	0.44	0.32	0.19	0.11	0.14	0.29	0.34	0.41	0.78	0.85	0.74	0.73	0.65	0.60	0.50	0.43	0.34	0.25
93	0.91	0.94	0.93	0.89	0.74	0.58	0.45	0.30	0.19	0.17	0.28	0.23	0.21	0.62	0.73	0.69	0.82	0.77	0.74	0.65	0.55	0.46	0.36
106	0.78	0.87	0.91	0.92	0.82	0.70	0.59	0.42	0.30	0.24	0.30	0.16	0.03	0.40	0.52	0.59	0.81	0.82	0.85	0.79	0.67	0.59	0.48
120	0.63	0.76	0.84	0.89	0.84	0.79	0.71	0.55	0.41	0.33	0.35	0.15	-0.04	0.21	0.32	0.46	0.72	0.78	0.87	0.87	0.77	0.73	0.59
137	0.49	0.64	0.75	0.83	0.85	0.85	0.80	0.68	0.52	0.44	0.45	0.19	-0.02	0.11	0.19	0.32	0.60	0.67	0.79	0.87	0.83	0.85	0.70
155	0.39	0.52	0.65	0.77	0.86	0.90	0.86	0.79	0.64	0.56	0.56	0.24	0.03	0.07	0.11	0.20	0.47	0.51	0.65	0.81	0.81	0.92	0.81
177	0.30	0.39	0.54	0.66	0.83	0.90	0.88	0.86	0.73	0.66	0.64	0.30	0.11	0.04	0.04	0.11	0.35	0.34	0.47	0.69	0.70	0.90	0.83
201	0.22	0.29	0.43	0.55	0.74	0.85	0.86	0.90	0.79	0.72	0.68	0.34	0.18	0.03	-0.00	0.08	0.27	0.23	0.33	0.57	0.55	0.80	0.77
228	0.18	0.22	0.35	0.45	0.65	0.76	0.82	0.90	0.83	0.76	0.68	0.36	0.21	0.04	-0.01	0.08	0.25	0.19	0.28	0.48	0.44	0.69	0.69
259	0.13	0.16	0.29	0.37	0.54	0.65	0.75	0.85	0.85	0.79	0.67	0.38	0.22	0.06	-0.03	0.09	0.25	0.15	0.24	0.41	0.34	0.57	0.61
295	0.11	0.12	0.25	0.32	0.47	0.57	0.68	0.80	0.83	0.78	0.64	0.39	0.22	0.07	-0.04	0.10	0.28	0.13	0.22	0.36	0.28	0.48	0.53
335	0.06	0.06	0.18	0.23	0.36	0.46	0.57	0.68	0.73	0.72	0.59	0.37	0.20	0.08	-0.06	0.07	0.26	0.10	0.15	0.28	0.19	0.34	0.47
382	0.07	0.07	0.18	0.22	0.34	0.43	0.53	0.63	0.68	0.69	0.57	0.37	0.21	0.09	-0.03	0.08	0.26	0.09	0.17	0.26	0.17	0.31	0.46

Previous cases had clear ridges of corr along integer q values for He and O.
Highest corr of lower energy Oxygen (130-300 keV) is at energies between a factor of 1-2 of H^+ energies - constant offset in energies of ~50 keV
Is this a mix of O^+ and O^{2+}? Probably not! Likely only O^+

Average kinetic energy gain:

$$E_{kin,avg} = 2\times\frac{1}{2}mv_{E\times B}^2$$

For a flow ~550 km/sec, leads to ~50 keV difference between H^+ and O^+

Summary

- Here we have shown 4 cases where we can use the correlation of flux between different energy channels of different species to deduce the charge state of highly suprathermal heavy ions in the magnetotail during substorm injections. These are representative of more the 50 cases we have identified with MMS-EIS data between 6-25 R_E
- At highly suprathermal energies (E $\gtrsim$ 200–300 keV) heavy ions (helium and oxygen) dominate proton flux
- Correlation analysis shows that these highly suprathermal energies are multiple charge-state solar wind ions, which are well ordered with H+ for constant E/q
- Thus, mass-dependent non-adiabatic acceleration is not necessary to explain the very highly energetic tails of these species
- Only shown for 1 case here, but ratio of pre- to post- enhancement fluxes are well-ordered by *E/q* for examples 1-3
- Evidence of cases with possible non-adiabatic “pick-up” energization, gives O+ an extra ~50 keV, but highest energy oxygen (>300) still primarily O^{6+}
- If you only take away one thing! Please don’t assume that “all-ion” measurements at highly suprathermal energies are H^+ or even singly charged, the spectral indices and energization you try to match in simulations won’t be right!

Sam.Bingham@jhuapl.edu

APL

JOHNS HOPKINS
APPLIED PHYSICS LABORATORY

Back-up Slides

Multiple ways to get E/q ordering:

Ukhorskiy et al. [2018] test particle+MHD – as ions are trapped in magnetic islands, energization due to steep magnetic field gradients. Still found E/q dependence, while energization could be non-adiabatic.

Mitchell et al. [2018] purely adiabatic acceleration within flow channel.

Catapano et al. (2017) - test particle simulation of ions under stochastic e-m perturbations in the current sheet, ion energization was proportional to charge state and only weakly dependent on ion mass ($\propto m^{1/5}$).

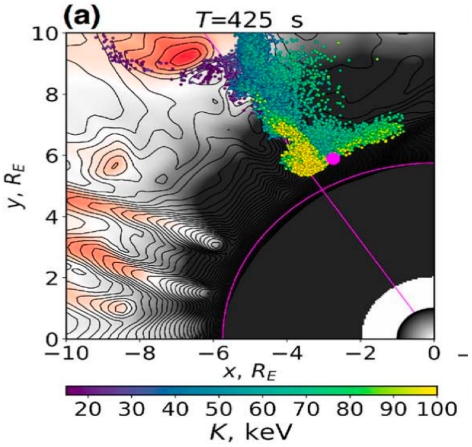

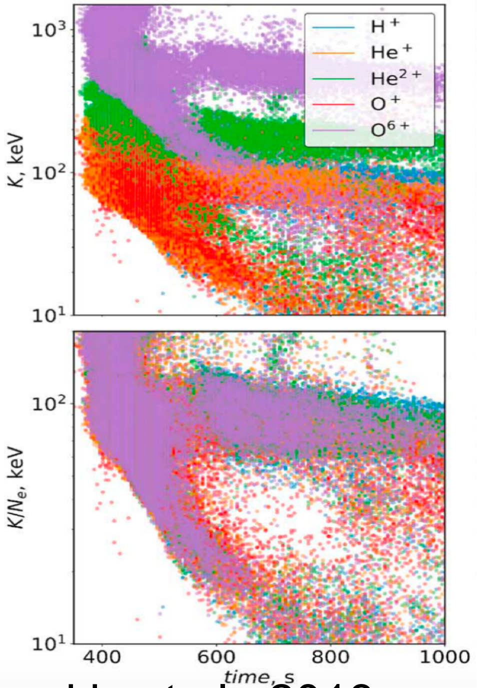

Ukhorskiy et al., 2018

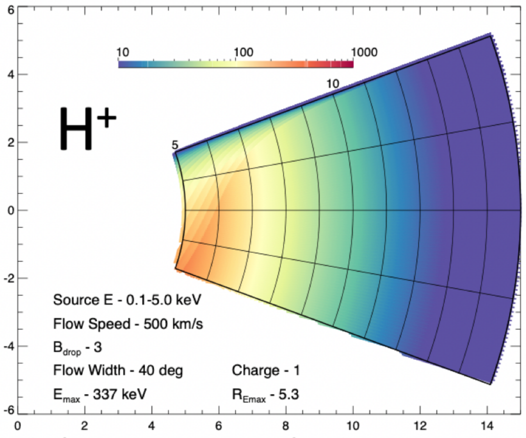

Source E - 0.1-5.0 keV

Flow Speed - 500 km/s

B_{drop} - 3

Flow Width - 40 deg

Charge - 1

E_{max} - 337 keV

R_{Emax} - 5.3

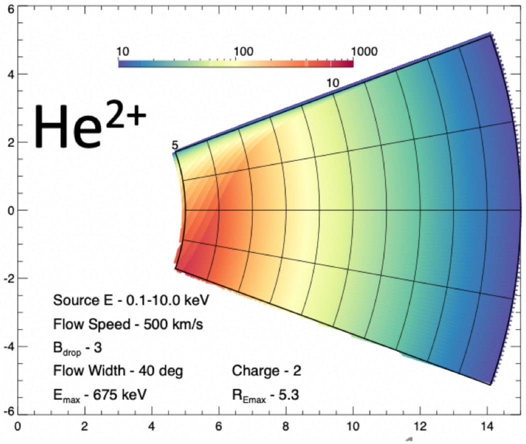

Source E - 0.1-10.0 keV

Flow Speed - 500 km/s

B_{drop} - 3

Flow Width - 40 deg

Charge - 2

E_{max} - 675 keV

R_{Emax} - 5.3